Preprints (www.preprints.org) | NOT PEER-REVIEWED | Posted: 2 October 2019 doi:10.20944/preprints201910.0023.v1

Peer-reviewed version available at *Geosciences* **2019**, *9*, 494; doi:10.3390/geosciences9120494

Article

Correlation of Elastic Moduli and Serpentine Content in Ultramafic Rocks

Aida Farough [1,*], Alexander Karrasch [1]

[1] Department of Geology, Kansas State University, Manhattan, KS

* Correspondence: afarough@ksu.edu

Abstract: Understanding the physical properties of ultramafic rocks is important for evaluating awide variety of petrologic models of the oceanic lithosphere, particularly upper mantle and lower crust. Hydration of oceanic peridotites results in increasing serpentine content, which affects lithospheric physical properties and the global bio/geochemical cycles of various elements. In understanding tectonic, magmatic and metamorphic history of the oceanic crust, interpreting seismic velocities, rock composition and elastic moduli are of fundamental importance.

In this study we show that as serpentine content increases, density decreases linearly with a slope of 7.85. We also correlate increase in serpentine content with a linear decline in shear, bulk and Young's moduli with slopes of 0.48, 0.77, 0.45 respectively. Our results show that increase in serpentine content of lower crust and forearc mantle could decrease elasticity of lithospehere and result in break-offs. Therefore tectonic processes at peridotite rich slow spreading ridges may be strongly affected by serpentine content, particularly serpentinization may be responsible for discontinuities in thin crust, and formation of weak fault zones.

Keywords: serpentinization; elastic moduli; density; ultramafic rocks; oceanic lithosphere

1. Introduction

Understanding the physical properties of ultramafic rocks (peridotites) is important for evaluating the wide variety of petrologic models for the Earth's upper mantle and lower oceanic crust [1].These properties have a key role in fluid flux and geochemical transport in magmatic system at mid oceanic ridges [e.g. 2-4] and subduction zones [e.g.5-6], as well as in enhanced geothermal systems [e.g. 7-8]. Mass, heat and chemical transport in fault zones plays a significant role in global seismicity [e.g. 9-10].

Hydration and alteration of oceanic peridotites results in increasing serpentine content and formation of serpentinites, which affects lithospheric physical properties [e.g.11-14] and the global bio/geo chemical cycles of various elements [e.g. 15-17].

In interpreting structure and seismic velocities of a region, a property of fundamental importance in understanding tectonic history is rock composition. Velocities of compressional and shear waves in ultramafic rocks decrease with increasing serpentine content [e.g. 18]. Various studies have reported seismic velocity measurements of dunites, partially serpentinized peroditites and serpentinites under pressure [e.g. 13, 19-25]. Falcon-Suarez et al., [26] analyzed seismic velocities, electrical resistivity and permeability of four serpentinized peridotite samples from the southern wall of the Atlantis Massif, Mid-Atlantic Ridge, collected during International Ocean

© 2019 by the author(s). Distributed under a Creative Commons CC BY license.

Preprints (www.preprints.org) | NOT PEER-REVIEWED | Posted: 2 October 2019 doi:10.20944/preprints201910.0023.v1

Peer-reviewed version available at Geosciences 2019, 9, 494; doi:10.3390/geosciences9120494

Discovery Program (IODP) Expedition 357. Horen et al., [27] analyzed the effect of serpentine content on seismic velocity of 6 samples from Xigaze Ophiolite and developed empirical correlations between the noted parameters, which we will use in this study to estimate seismic velocities. Ramana and Rao [28] reports density, porosity and seismic velocity of fresh (12%) to extensively altered ultramafic rocks (100%) from India.

Elastic moduli are also important in evaluating stiffness and understanding the tectonic, magmatic and metamorphic history of the oceanic crust. Evaluation of elastic moduli of oceanic rocks can be beneficial for future drilling strategies [13]. mineralogical composition, the porosity and the texture of the rocks are some of the parameter that affect elastic moduli [26, 28].

In this paper we report density, porosity and serpentine content of 8 samples of slightly to extensively serpentinized rocks and develop a linear correlation between density and serpentine content. We also use the empirical equation of Horen et al., [27], to estimate seismic velocities of the samples used in this study and develop correlation between elastic moduli and serpentine content. We produce a series of linear functions that correlate serpentine content with elastic moduli. These models can be used in understanding tectonic evolution of oceanic crust and estimating crustal weakening as a result of serpentinization.

Although the elastic thickness of the oceanic lithosphere, is estimated in the range of 2-50 km [29], serpentinization of lower crust and upper mantle can result in reduction of elasticity and weakening at much shallower depths, depending on fluid access. Serpentinization will impact onset of brittle failure or dilatancy in the lower crust and upper mantle, forming weak faults and a brittle crust, in response to bending stresses and seismicity. Serpentine content is one of the factors that affect the amount of weakening resulting from the alteration of peridotite to serpentinite [12, 30].

2. Materials and Methods

The measurements were performed on cubes (7.3-13.1 cm^3) and mini cores (1.8-2.7 cm^3) of serpentinized dunites, pyroxenites and peridotites. The major phase of each sample and serpentine content estimated through petrographic analysis is provided in Table 1. Figure (1) contains photomicrographs of each sample in plain polarized (PPL) and crossed polarized (XPL) light. Three samples, denoted by symbols TS, JC, and ND respectively, are dunites from the Twin Sisters Range in Washington (Figure 1(a), (b)), Jackson County in North Carolina (Figure 1(e), (f)), and Newdale from the Blue Ridge province in North Carolina (Figure 1(g), (h)), respectively. They contain 60-95% Mg-rich olivine, the remainder composed of serpentine and 5% of minor minerals. One sample (BC) is a pyroxenite from the Bushveld Complex, South Africa (Figure 1(c), (d)), containing more than 90% Mg-rich orthopyroxene, about 10% serpentine, and 5% other minor minerals. Four samples were selected from the Point Sal Ophiolite in California (Figure 1(i), (j), (k), (l), (m), (n), (o), (p)) with major phase of Serpentine composing 60-95% of the samples, with various other minor phases including olivine and pyroxene.

Densities were calculated from the dimensions and weights of the cubes and mini cores. Porosity of the samples were measured by saturation under vacuum conditions, with the triple weighing technique similar to the method of Saad [31]. The serpentine content was estimated by petrographic analysis.

Preprints (www.preprints.org) | NOT PEER-REVIEWED | Posted: 2 October 2019 doi:10.20944/preprints201910.0023.v1

Peer-reviewed version available at Geosciences 2019, 9, 494; doi:10.3390/geosciences9120494

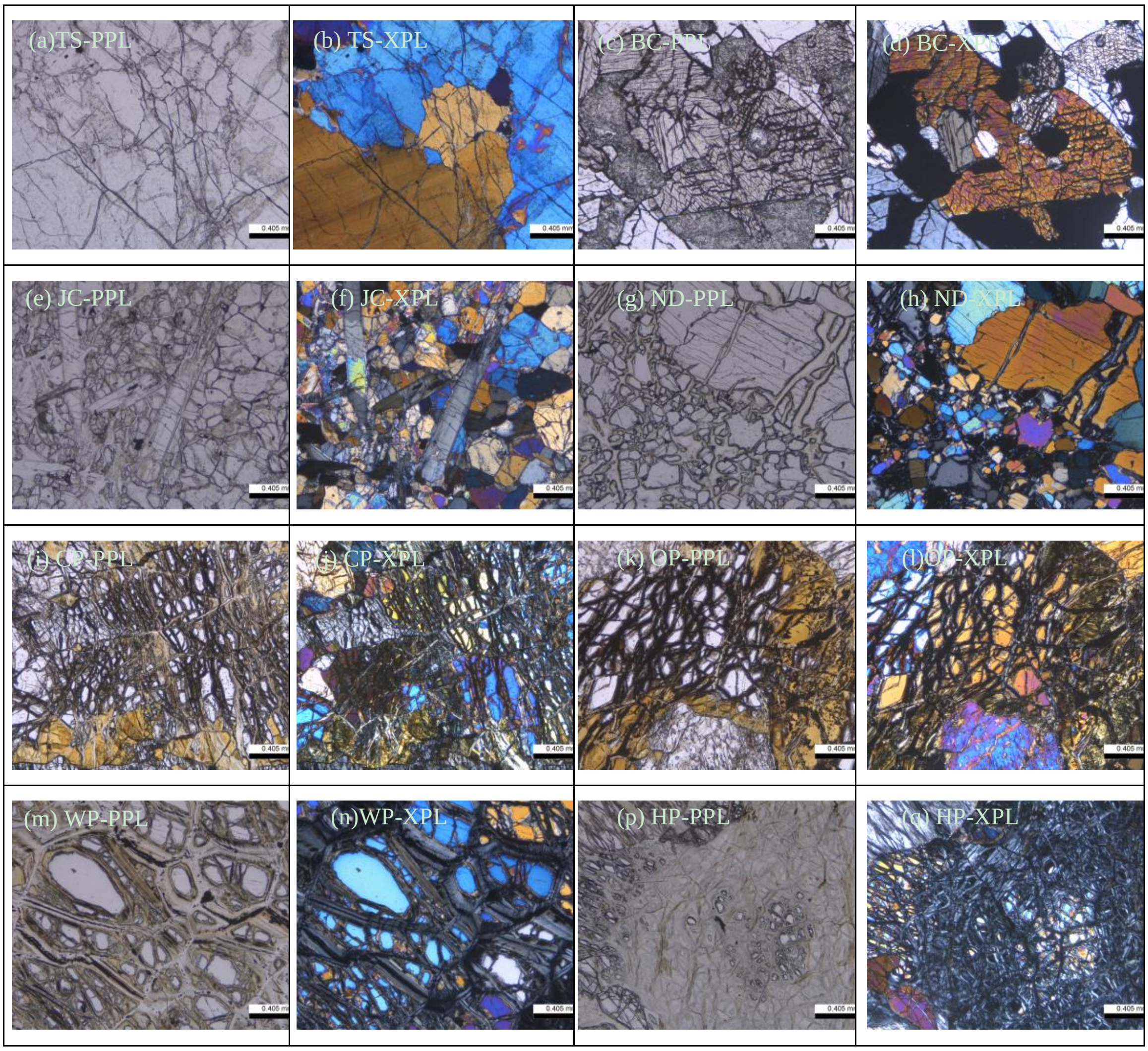

Figure 1. Photomicrographs of the samples in the order of increasing serpentine content. PPL=Plain Polarized Light, XPL=Crossed Polarized Light. In all the images veins of serpentine in olivine and pyroxene are visible.

3. Results

3.1. Measurements of Density and Porosity

Measured bulk density ρ values ranged between 2540 kg/m³ for HP sample to 3200 kg/m³ for TS sample. The porosity of the samples ranges between 2.1% in the WP sample to 8.4% in ND sample (Table 2). Using measurements of bulk density and porosity, the grain density was estimated to range between 2644 kg/m³ for HP sample to 3328 kg/m³ for TS sample, which matches with the density of serpentine and un-serpentinized dunite respectively.

3.1.1.Density Variation with Serpentine Content

To find the best fit for ρ -β correlation, we added published data from Falcon-Suarez et al., [26], Ramana and Rao, [28] and Horen et al., [27] to our data. In all of the above studies, β is

Preprints (www.preprints.org) | NOT PEER-REVIEWED | Posted: 2 October 2019 doi:10.20944/preprints201910.0023.v1

Peer-reviewed version available at Geosciences 2019, 9, 494; doi:10.3390/geosciences9120494

estimated by petrographic analysis. As shown in Figure (2) increase in β result in linear decline in ρ following equation (1):

$$\beta \times 7.85 = \rho_{peridotite} - \rho_{bulk} \quad (1)$$

where $\rho_{peridotite}$=3300 kg/m³. The R2 for this equation is 0.82. Miller and Christensen [13] report the same correlation between ρ and β of various serpentinized harzburgites and dunites from around the world with R2=0.98.

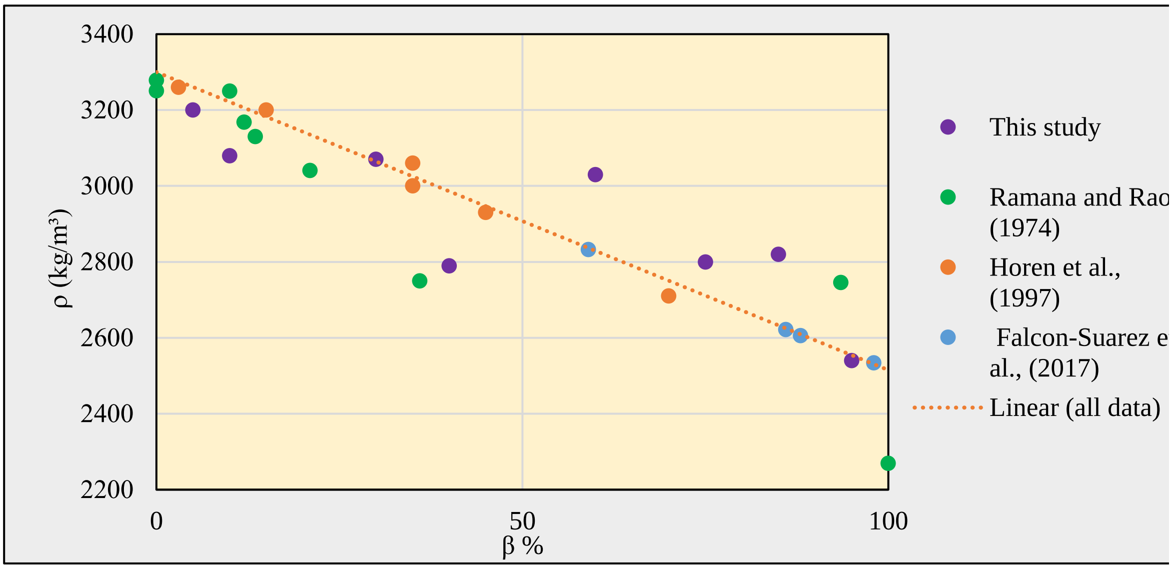

Figure 2. The assumptions of the linear correlation between density and serpentine content is that serpentine content of peridotite with density of 3300 kg/m³ is 0 and serpentine content of serpentinite with density of 2500 kg/m³ is 100%.

Porosity of the samples does not correlate systematically with serpentine content. This could be resulted from tectonic and erosional processes affecting porosity well beyond the impact of serpentinization.

3.2. Estimating Seismic Velocities

Various previous studies have proven a linear correlation between seismic velocities and serpentine content [13, 20, 25]. The empirical correlation between Compressional Velocity V_p and Shear Velocity V_s with serpentine content developed in Horen et al., [27]:

$$V_p = (7922 - 32.5\beta)\ m/s \quad (2)$$
$$V_s = (4371 - 21.8\beta)\ m/s \quad (3)$$

where β refers to serpentine content. V_p and V_s values of the samples in this study were estimated in range of 4834.5-7759.5 m/s for V_p and 2300-4262 m/s for V_s of HP and TS samples respectively

Preprints (www.preprints.org) | NOT PEER-REVIEWED | Posted: 2 October 2019 doi:10.20944/preprints201910.0023.v1

Peer-reviewed version available at Geosciences 2019, 9, 494; doi:10.3390/geosciences9120494

(Table 3). Based on the data published in Christensen [1], the VP/Vs ratio is showing that most samples are possibly rich in Lizardite serpentine (Table 3).
Previous studies show serpentinized peridotites of Point Sal have compressional velocities around 5.5 km/s [18], which agrees with our estimates.

3.3. Estimating Elastic Moduli and Poisson's Ratio

Elastic moduli are correlated with seismic velocities, based on equations below:

$$\mu = \rho V_s^2 \quad (4)$$
$$K = \rho V_p^2 - 1.33\mu \quad (5)$$
$$E = \rho(V_p^2 - 2V_s^2) \quad (6)$$
$$\nu = \frac{V_p^2 - 2V_s^2}{2(V_p^2 - V_s^2)} \quad (7)$$

where μ is shear modulus or rigidity, K is bulk modulus or incompressibility, E is Young's modulus and ν is Poisson's ratio. By incorporating results of equations (2) and (3) into (4), (5), (6) and (7), μ is estimated between 13.4-58.1 GPa, K is estimated between 41.5-115 GPa, and E is estimated between 32.5-76.4 GPa for HP and TS samples respectively. Estimated values of ν ranges from 0.28 for the TS sample to 0.35 for the HP sample (Table 3). High ν is as a result of low shear wave velocities in serpentinized ultramafic rocks, which agrees with previous studies [1, 32,].

3.3.1. Elastic Moduli Variation with Serpentine Content

As shown in Figure 3 with increase in serpentine content, μ, K and E will decrease linearly following equations (8), (9) and (10):

$$\mu = -0.48\beta + \mu_0 \quad (8)$$
$$K = -0.77\beta + K_0 \quad (9)$$
$$E = -0.45\beta + E_0 \quad (10)$$

where subscript 0 refers to a fresh peridotite where $\beta = 0$, $\mu_0 = 57.6$, $K_0 = 115$ and $E_0 = 76.6$. μ_0 and K_0 values are in agreement with reported values in Christensen [19], Christensen and Shaw [34], Christensen [20] and Turcotte and Schubert, [35]. The R2 of equations (8), (9) and (10) is 0.98.

Preprints (www.preprints.org) | NOT PEER-REVIEWED | Posted: 2 October 2019 doi:10.20944/preprints201910.0023.v1

Peer-reviewed version available at *Geosciences* **2019**, *9*, 494; doi:10.3390/geosciences9120494

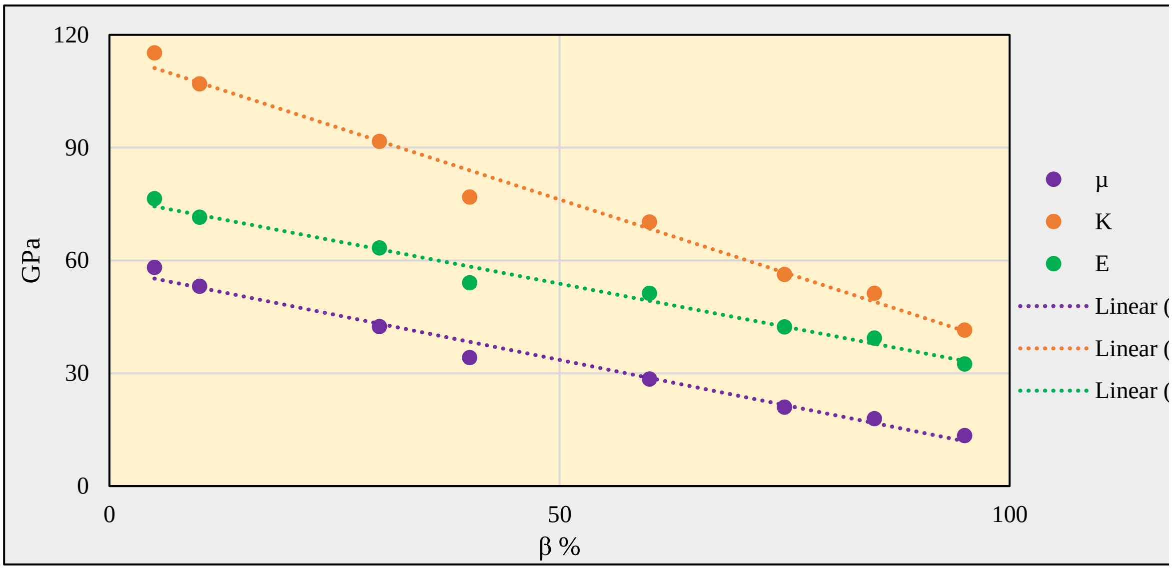

Figure 3. Shows the trend of Elastic Moduli (μ, K and E) with serpentine content

The standard deviation of μ, K and E (Table 4, Figure 4) was calculated by estimating the elastic moduli of Horen et al., [27] samples using the measured seismic velocities in comparison to estimating the equations above.

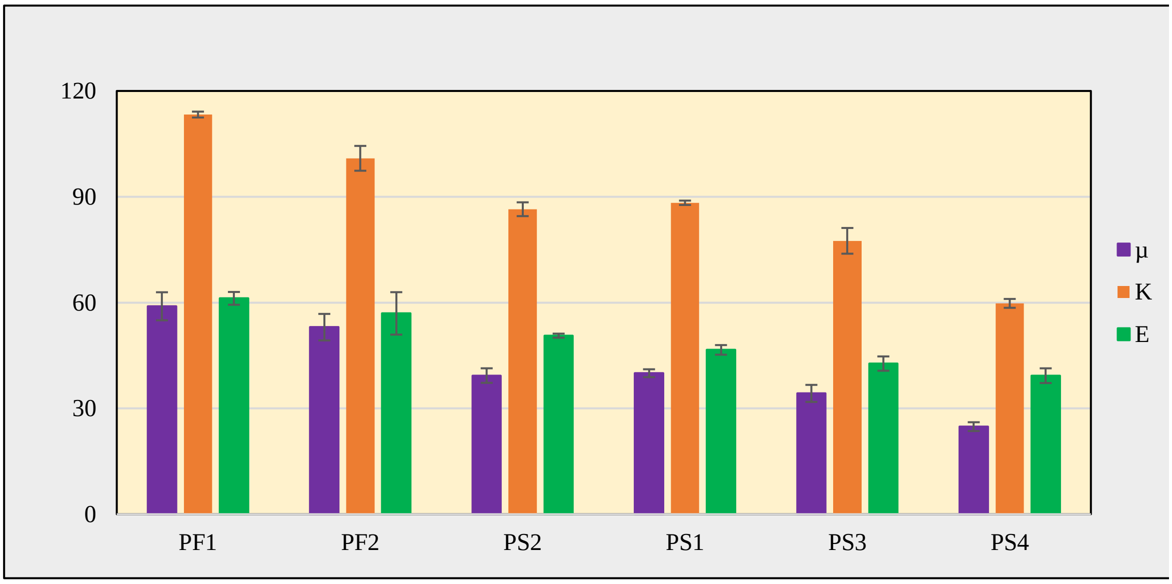

Figure 4. The bars show the mean value of elastic moduli from Table 4 and the error bars represent the standard deviation (STD) from Table 4 for Horen et al., [27] samples.

4. Discussion

Our results show that increase in serpentine content will result in a linear decrease in density, and elastic moduli, which is in agreement with results of Christensen [19]. Our calculated elastic moduli of HP samples which is 95% serpentinized, is in great agreement with that for serpentinites

Preprints (www.preprints.org) | NOT PEER-REVIEWED | Posted: 2 October 2019 doi:10.20944/preprints201910.0023.v1

Peer-reviewed version available at Geosciences 2019, 9, 494; doi:10.3390/geosciences9120494

reported in Christensen [1972] and Carlson [36]. This agreement is slightly weaker between our freshest sample, TS, which is a slightly serpentinized dunite compared to estimates of fresh oceanic peridotite of Christensen [20], as a result of compositional difference between serpentinized dunite and oceanic peridotite.

Our results show that increase in serpentine content of lower crust and forearc mantle could decrease elasticity of lithospehere and result in break-offs [e.g. 12, 30, 33, 37].

Therefore tectonic processes at peridotite rich slow spreading ridges may be strongly affected by serpentine content, particularly serpentinization may be responsible for observed discontinuities in thin crust, and formation of weak fault zones [e.g. 12, 38, 39, 40].

5. Conclusions

In this study we show that as serpentine content increases, density decreases linearly with a slope of 7.85. We also correlate increase in serpentine content with a linear decline in shear, bulk and Young's moduli with slopes of 0.48, 0.77, 0.45 respectively. Compositional variations with lower serpentine content ultramafic rocks, can result in variation of elastic moduli.

Our results show that increase in serpentine content of lower crust and forearc mantle could decrease elasticity of lithospehere and result in break-offs. Therefore tectonic processes at peridotite rich slow spreading ridges may be strongly affected by serpentine content, particularly serpentinization may be responsible for formation of discontinuities in thin crust, and weak fault zones.

Tables

Table 1. Description of the samples used for the experiments.

Name	label	Major phase	Serpentine content β %
Twin Sisters dunite	TS	Olivine	5
Bushveld Complex pyroxenite	BC	Pyroxene	10
Jackson County dunite	JC	Olivine	30
Newdale dunite	ND	Olivine	40
Point Sal sample 1	CP	Serpentine	60
Point Sal sample 2	OP	Serpentine	75
Point Sal sample 3	WP	Serpentine	85
Point Sal sample 4	HP	Serpentine	95

Table 2. Measurements of density and porosity and estimates of grain density.

Sample	ρ kg/m3	φ %	ρs kg/m3
TS	3200	3.8	3328
BC	3080	2.3	3152
JC	3070	2.7	3154
ND	2790	8.4	3047
CP	3030	2.3	3102
OP	2800	4.9	2944
WP	2820	2.1	2881

Preprints (www.preprints.org) | NOT PEER-REVIEWED | Posted: 2 October 2019 doi:10.20944/preprints201910.0023.v1

Peer-reviewed version available at Geosciences 2019, 9, 494; doi:10.3390/geosciences9120494

HP	2540	3.9	2644

Table 3. Calculated seismic velocities and elastic moduli. Seismic velocities are calculated based on equations (1) and (2) for Vp and Vs and elastic moduli are calculated based on equations (3), (4), (5) and (6) for μ, K and E and ν respectively.

Sample	Vp (m/s)	Vs (m/s)	Vp/Vs	μ (GPa)	K (GPa)	E (GPa)	ν
TS	7759.5	4262	1.82	58.1	115	76.4	0.28
BC	7597	4153	1.83	53.1	107	71.5	0.28
JC	6947	3717	1.87	42.4	91.6	63.3	0.29
ND	6622	3499	1.89	34.2	76.8	54.03	0.30
CP	5972	3063	1.95	28.4	70.2	51.2	0.32
OP	5484.5	2736	2.00	21.0	56.3	42.3	0.33
WP	5159.5	2518	2.05	17.9	51.2	39.3	0.34
HP	4834.5	2300	2.10	13.4	41.5	32.5	0.35

Table 4. Seismic velocities and elastic moduli of Horen et al., (1996) samples.

Horen et al., [27] samples	V_p (m/s)	V_s (m/s)	μ* (Gpa)	μ** (Gpa)	mean	STD	K* (Gpa)	K** (Gpa)	mean	STD	E* (Gpa)	E** (Gpa)	mean	STD
PF1	7759	4353	61.77	56.15	58.96	3.98	113.90	112.72	113.31	0.83	72.71	75.28	61.20	1.81
PF2	7346	4172	55.70	50.38	53.04	3.76	98.42	103.40	100.91	3.52	61.29	69.80	56.94	6.02
PS2	6722	3552	37.85	40.77	39.31	2.07	85.09	87.86	86.47	1.96	59.86	60.67	50.62	0.58
PS1	6788	3579	39.20	40.77	39.98	1.11	88.73	87.86	88.30	0.62	62.60	60.67	46.59	1.37
PS3	6355	3333	32.55	35.97	34.26	2.42	74.93	80.09	77.51	3.65	53.23	56.10	42.71	2.03
PS4	5864	3081	25.72	23.95	24.84	1.25	58.89	60.67	59.78	1.26	41.74	44.69	39.28	2.09

1) μ*, K* and E* are calculated using Vp and Vs based on equations (4), (5), (6) respectively

2) μ**, K** and E** are calculated using equations (8), (9) and (10) respectively

Preprints (www.preprints.org) | NOT PEER-REVIEWED | Posted: 2 October 2019 doi:10.20944/preprints201910.0023.v1

Peer-reviewed version available at *Geosciences* **2019**, *9*, 494; doi:10.3390/geosciences9120494

Author Contributions: conceptualization, A.F..; methodology, A.F.; formal analysis, A.F.; investigation, A.K.; resources, A.F.; data curation, A.K.; writing—original draft preparation, A.F.; writing—review and editing, A.F.; visualization, A.F.; supervision, A.F.; project administration, A.F.

Acknowledgments: All the data are provided in Tables section of this manuscript. The authors would like to thank Kayleigh Rogers for help with petrographic analysis. We are also thankful to William Dinklage for providing the Point Sal samples. Authors would also like to acknowledge help and support from Dr. Robert P. Lowell (deceased) on earlier versions of this manuscript.

Conflicts of Interest: The authors declare no conflict of interest.

Preprints (www.preprints.org) | NOT PEER-REVIEWED | Posted: 2 October 2019 doi:10.20944/preprints201910.0023.v1

Peer-reviewed version available at Geosciences 2019, 9, 494; doi:10.3390/geosciences9120494

References

1. Christensen, N. I. (2004). Serpentinites, peridotites, and seismology. *International Geology Review*, *46*(9), 795-816. https://doi.org/10.2747/0020-6814.46.9.795
2. Lowell, R. P., Circulation in fractures, hot springs, and convective heat transport on mid-ocean ridge crests, *Geophysical Journal of the Royal Astronomical Society*,40, 351–365, 1975. https://doi.org/10.1111/j.1365-246X.1975.tb04137.x
3. Bickle, M. J., & Teagle, D. A. (1992). Strontium alteration in the Troodos ophiolite: implications for fluid fluxes and geochemical transport in mid-ocean ridge hydrothermal systems. *Earth and Planetary Science Letters*, *113*(1-2), 219-237. https://doi.org/10.1016/0012-821X(92)90221-G
4. Elderfield, H., Wheat, C. G., Mottl, M. J., Monnin, C., & Spiro, B. (1999). Fluid and geochemical transport through oceanic crust: a transect across the eastern flank of the Juan de Fuca Ridge. *Earth and Planetary Science Letters*, *172*(1-2), 151-165. https://doi.org/10.1016/S0012-821X(99)00191-0
5. Hyndman, R. D., & Wang, K. (1993). Thermal constraints on the zone of major thrust earthquake failure: The Cascadia subduction zone. *Journal of Geophysical Research: Solid Earth*, *98*(B2), 2039-2060. **https://doi.org/10.1029/92JB02279**
6. Gamage, K., Screaton, E., Bekins, B., & Aiello, I. (2011). Permeability–porosity relationships of subduction zone sediments. *Marine Geology*, *279*(1-4), 19-36. https://doi.org/10.1016/j.margeo.2010.10.010
7. Pruess, K. (2006). Enhanced geothermal systems (EGS) using CO2 as working fluid—A novel approach for generating renewable energy with simultaneous sequestration of carbon. *Geothermics*, *35*(4), 351-367. https://doi.org/10.1016/j.geothermics.2006.08.002
8. Taron, J., & Elsworth, D. (2009). Thermal–hydrologic–mechanical–chemical processes in the evolution of engineered geothermal reservoirs. *International Journal of Rock Mechanics and Mining Sciences*, *46*(5), 855-864. https://doi.org/10.1016/j.ijrmms.2009.01.007
9. Byerlee, J. D. (1993). Model for episodic flow of high-pressure water in fault zones before earthquakes. *Geology*, *21*(4), 303-306. https://doi.org/10.1130/0091-7613(1993)021<0303:MFEFOH>2.3.CO;2
10. Sleep, N. H., & Blanpied, M. L. (1994). Ductile creep and compaction: A mechanism for transiently increasing fluid pressure in mostly sealed fault zones. *Pure and Applied Geophysics*, *143*(1-3), 9-40.
11. O'Hanley, D. S. (1992). Solution to the volume problem in serpentinization. *Geology*, *20*(8), 705-708. https://doi.org/10.1130/0091-7613(1992)020<0705:STTVPI>2.3.CO;2
12. Escartin, J., Hirth, G., & Evans, B. (1997). Nondilatant brittle deformation of serpentinites: Implications for Mohr-Coulomb theory and the strength of faults. *Journal of Geophysical Research: Solid Earth*, *102*(B2), 2897-2913. **https://doi.org/10.1029/96JB02792**
13. Miller, D. J., & Christensen, N. I. (1997). Seismic velocities of lower crustal and upper mantle rocks from the slow-spreading Mid-Atlantic Ridge, south of the Kane Transform Zone (MARK). In *PROCEEDINGS-OCEAN DRILLING PROGRAM SCIENTIFIC RESULTS* (pp. 437-456). NATIONAL SCIENCE FOUNDATION.
14. Oufi, O., Cannat, M., & Horen, H. (2002). Magnetic properties of variably serpentinized abyssal peridotites. *Journal of Geophysical Research: Solid Earth*, *107*(B5), EPM-3. **https://doi.org/10.1029/2001JB000549**
15. Früh-Green, G. L., Connolly, J. A., Plas, A., Kelley, D. S., & Grobéty, B. (2004). Serpentinization of oceanic peridotites: implications for geochemical cycles and biological activity. *The subseafloor biosphere at mid-ocean ridges*, *144*, 119-136.
16. Paulick, H., Bach, W., Godard, M., De Hoog, J. C. M., Suhr, G., & Harvey, J. (2006). Geochemistry of abyssal peridotites (Mid-Atlantic Ridge, 15 20′ N, ODP Leg 209): implications for fluid/rock interaction in slow spreading environments. *Chemical Geology*, *234*(3-4), 179-210. https://doi.org/10.1016/j.chemgeo.2006.04.011

Preprints (www.preprints.org) | NOT PEER-REVIEWED | Posted: 2 October 2019 doi:10.20944/preprints201910.0023.v1

Peer-reviewed version available at *Geosciences* **2019**, *9*, 494; doi:10.3390/geosciences9120494

17. Deschamps, F., Godard, M., Guillot, S., & Hattori, K. (2013). Geochemistry of subduction zone serpentinites: A review. *Lithos*, *178*, 96-127. https://doi.org/10.1016/j.lithos.2013.05.019
18. Nichols, J., Warren, N., Luyendyk, B. P., & Spudich, P. (1980). Seismic velocity structure of the ophiolite at Point Sal, southern California, determined from laboratory measurements. *Geophysical Journal International*, *63*(1), 165-185. https://doi.org/10.1111/j.1365-246X.1980.tb02615.x
19. Christensen, N. I. (1966). Elasticity of ultrabasic rocks. *Journal of Geophysical Research*, *71*(24), 5921-5931. **https://doi.org/10.1029/JZ071i024p05921**
20. Christensen, N. I. (1972). The abundance of serpentinites in the oceanic crust. *The Journal of Geology*, *80*(6), 709-719. https://doi.org/10.1086/627796
21. Christensen, N. I. (1978). Ophiolites, seismic velocities and oceanic crustal structure. *Tectonophysics*, *47*(1-2), 131-157.https://doi.org/10.1016/0040-1951(78)90155-5
22. Schreiber, E., & Fox, P. J. (1977). Density and P-wave velocity of rocks from the FAMOUS region and their implication to the structure of the oceanic crust. *Geological Society of America Bulletin*, *88*(4), 600-608.https://doi.org/10.1130/0016-7606(1977)88<600:DAPVOR>2.0.CO;2
23. Christensen, N. I., & Smewing, J. D. (1981). Geology and seismic structure of the northern section of the Oman ophiolite. *Journal of Geophysical Research: Solid Earth*, *86*(B4), 2545-2555. **https://doi.org/10.1029/JB086iB04p02545**
24. Iturrino, G. J., Miller, D. J., & Christensen, N. I. (1996). 25. VELOCITY BEHAVIOR OF LOWER CRUSTAL AND UPPER MANTLE ROCKS FROM A FAST-SPREADING RIDGE AT HESS DEEP1.
25. Escartin, J., Hirth, G., & Evans, B. (2001). Strength of slightly serpentinized peridotites: Implications for the tectonics of oceanic lithosphere. *Geology*, *29*(11), 1023-1026. https://doi.org/10.1130/0091-7613(2001)029<1023:SOSSPI>2.0.CO;2
26. Falcon-Suarez, I., Bayrakci, G., Minshull, T. A., North, L. J., Best, A. I., Rouméjon, S., & IODP Expedition 357 Science Party. (2017). Elastic and electrical properties and permeability of serpentinites from Atlantis Massif, Mid-Atlantic Ridge. *Geophysical Journal International*, *211*(2), 686-699. https://doi.org/10.1093/gji/ggx341
27. Horen, H., Zamora, M., & Dubuisson, G. (1996). Seismic waves velocities and anisotropy in serpentinized peridotites from Xigaze ophiolite: abundance of serpentine in slow spreading ridge. *Geophysical Research Letters*, *23*(1), 9-12. **https://doi.org/10.1029/95GL03594**
28. Ramana, Y. V., & Rao, M. V. M. S. (1974). Compressional velocities in ultramafic rocks of India at pressures to five kilobars. *Geophysical Journal International*, *37*(1), 207-212. https://doi.org/10.1111/j.1365-246X.1974.tb02453.x
29. Watts, A. B., & Burov, E. B. (2003). Lithospheric strength and its relationship to the elastic and seismogenic layer thickness. *Earth and Planetary Science Letters*, *213*(1-2), 113-131. https://doi.org/10.1016/S0012-821X(03)00289-9
30. Brace, W. F., Paulding Jr, B. W., & Scholz, C. H. (1966). Dilatancy in the fracture of crystalline rocks. *Journal of Geophysical Research*, *71*(16), 3939-3953. **https://doi.org/10.1029/JZ071i016p03939**
31. Saad, A. H. (1969). Magnetic properties of ultramafic rocks from Red Mountain, California. *Geophysics*, *34*(6), 974-987. https://doi.org/10.1190/1.1440067
32. Reynard, B., Hilairet, N., Balan, E., & Lazzeri, M. (2007). Elasticity of serpentines and extensive serpentinization in subduction zones. *Geophysical Research Letters*, *34*(13). **https://doi.org/10.1029/2007GL030176**
33. Bostock, M. G., Hyndman, R. D., Rondenay, S., & Peacock, S. M. (2002). An inverted continental Moho and serpentinization of the forearc mantle. *Nature*, *417*(6888), 536. https://doi.org/10.1038/417536a
34. Christensen, N. I., & Shaw, G. H. (1970). Elasticity of mafic rocks from the Mid-Atlantic Ridge. *Geophysical Journal International*, *20*(3), 271-284. https://doi.org/10.1111/j.1365-246X.1970.tb06070.x
35. Turcotte, D., & Schubert, G. (2014). *Geodynamics*. Cambridge university press.

Preprints (www.preprints.org) | NOT PEER-REVIEWED | Posted: 2 October 2019 doi:10.20944/preprints201910.0023.v1

Peer-reviewed version available at *Geosciences* **2019**, *9*, 494; doi:10.3390/geosciences9120494

36. Carlson, R. L. (2001). The abundance of ultramafic rocks in Atlantic Ocean crust. *Geophysical Journal International*, *144*(1), 37-48. https://doi.org/10.1046/j.0956-540X.2000.01280.x
37. Gerya, T. V., Yuen, D. A., & Maresch, W. V. (2004). Thermomechanical modelling of slab detachment. *Earth and Planetary Science Letters*, *226*(1-2), 101-116. https://doi.org/10.1016/j.epsl.2004.07.022
38. Tolstoy, M., Harding, A. J., & Orcutt, J. A. (1993). Crustal thickness on the Mid-Atlantic Ridge: Bull's-eye gravity anomalies and focused accretion. *Science*, *262*(5134), 726-729. DOI: 10.1126/science.262.5134.726
39. Tucholke, B. E., & Lin, J. (1994). A geological model for the structure of ridge segments in slow spreading ocean crust. *Journal of Geophysical Research: Solid Earth*, *99*(B6), 11937-11958. **https://doi.org/10.1029/94JB00338**
40. Cannat, M., Mevel, C., Maia, M., Deplus, C., Durand, C., Gente, P., ... & Reynolds, J. (1995). Thin crust, ultramafic exposures, and rugged faulting patterns at the Mid-Atlantic Ridge (22–24 N). *Geology*, *23*(1), 49-52. https://doi.org/10.1130/0091-7613(1995)023<0049:TCUEAR>2.3.CO;2